

High Sensitivity Torsion Balance Tests for LISA Proof Mass Modeling

S. Schlamminger, C. A. Hagedorn, M. G. Famulare, S. E. Pollack and
J. H. Gundlach

*Department of Physics, Center for Experimental Nuclear Physics and Astrophysics, Box 354290,
University of Washington, Seattle, WA, 98195-4290*

Abstract. We have built a highly sensitive torsion balance to investigate small forces between closely spaced gold coated surfaces. Such forces will occur between the LISA proof mass and its housing. These forces are not well understood and experimental investigations are imperative. We describe our torsion balance and present the noise of the system. A significant contribution to the LISA noise budget at low frequencies is the fluctuation in the surface potential difference between the proof mass and its housing. We present first results of these measurements with our apparatus.

Keywords: LISA, torsion balance, contact potential, force noise

PACS: 04.80.Nn, 07.10.Pz, 95.55.Ym

INTRODUCTION

One of the leading contributions to the LISA acceleration noise budget at frequencies below 1 mHz is electrostatic force noise acting on the proof mass [1, 2, 3]. Very little is known about spurious electrostatic forces that arise between two conducting surfaces.

We have built a highly sensitive torsion balance apparatus to measure small forces which may act between closely spaced surfaces. We introduce our instrument, its performance and an investigations of these electrostatic forces.

EXPERIMENTAL SETUP

Our instrument consists of a vertical planar metal surface parallel to which we suspend a thin plate from a thin wire. The latter plate is designed to emulate LISA's proof mass housing surface and the opposing metal surface has properties which are similar to those of the proof mass. The suspended thin plate forms a torsion pendulum which is exquisitely sensitive to small forces.

The main body of the pendulum plate is a rectangular section, cut from a 0.43 mm thick silicon wafer, which is $l = 114.3$ mm long and $h = 38.1$ mm high. At the center the plate has another smaller rectangular section, 25.4 mm long and 34.9 mm high, so that the pendulum has the shape of an upside-down T. At the top of the pendulum plate an aluminum compensator bar is attached perpendicular to the plate. This bar was designed to minimize the gravitational quadrupole moment of the pendulum in order to reduce the sensitivity to mass movements in its vicinity. A tungsten torsion fiber is attached to the compensator bar. The fiber is 0.534 m long and has a diameter of 13 μm which provides

a restoring torque of $\kappa = 774$ pNm/rad.

The entire pendulum is gold coated. The silicon plate was coated with an adhesion layer of 20 nm TiW shortly after it was dipped into hydrofluoric acid to remove the natural oxide layer. A 225 nm thick gold coating gold was sputtered onto the adhesion layer.

The metal plate parallel to the pendulum plate is mounted on a translation stage to vary its separation from the pendulum between 0 mm to 10 mm. This plate is machined from OFHC copper. It is larger than the main plate of the pendulum: 50.8 mm high and 127.5 mm wide. The copper plate is split into two halves. The halves are separated by a 0.5 mm gap to isolate them electrically and thermally from one another. To each copper plate an electrostatic potential can be independently applied. Each half of the copper plate has a 600 mW resistive heater built-in and is equipped with a temperature sensor.

The two half of the copper plates have been coated by a sputtering process similar to the one used for the pendulum. In order to prevent the gold from diffusing into the copper we used TiW as a diffusion barrier.

In order to control the torsional motion of the pendulum, two electrodes (right and left) were installed near the back of the pendulum plate (see Figure 1 for a top view of the geometry). These electrodes are small (25 mm by 40 mm high) and far enough away (≈ 6 mm) that they do not cause any excess noise. On each electrode a voltage can be independently applied. The pendulum itself is grounded through the torsion fiber which has a resistance of 270 Ω .

The rotational angle of the pendulum is measured with an autocollimator. The infrared autocollimator beam passes through a glass window into the vacuum chamber and is reflected off the pendulum twice before it is returned to the autocollimator. The return beam is focused onto a position-sensitive photo-detector.

The pendulum and the plate are in a stainless steel vacuum chamber that is maintained with a turbo-molecular pump at $\approx 10^{-5}$ Pa. Systematic studies of pressure-related effects were done by changing the rotation rate of the turbo pump [4].

The actuator for translating the copper plate is located outside the vacuum chamber and has a resolution of 0.001 mm. In order to measure the absolute distance between the pendulum and the plate three different methods were used: (A) the plate was moved near the pendulum and the clockwise and counterclockwise deflection angles at which the pendulum touched the copper plate were measured. For a given distance the maximum deflection angle is given by half the length of the pendulum divided by the separation. (B) a window on the bottom of the vacuum chamber accommodates imaging of the pendulum with a CCD camera. The separation can be inferred from the video image. (C) we measured the capacitance between the pendulum and the copper plate as a function of distance. By fitting the function $C(x) = A/(x - x_o) + C_p$ we fit for the distance x_o . The parasitic capacitance C_p can be established by moving the plate far away from the pendulum.

The apparatus rests on a thick copper plate and is located inside two layers of styro-foam. The instrument is located on a deep foundation in a thermally stabilized room.

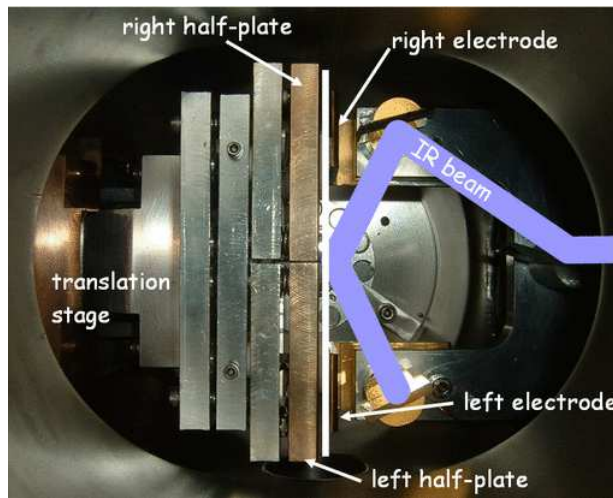


FIGURE 1. Annotated photograph of the plate and electrode layout. The pendulum has been removed to take this picture. The pendulum would be suspended in the space between the copper plate and the electrodes, indicated by the white line. For this picture, however, the plate was moved a few mm beyond the pendulum's position. The light gray trace schematically shows the beam path of the autocollimator located to the right outside the vacuum vessel.

MEASUREMENTS

In order to measure torques on the pendulum we employ two different methods.

In the so-called free-run mode, the pendulum is allowed to move freely and the torsional angle as a function of time is recorded. This mode is used to assess the baseline noise of the system, i.e. at plate-pendulum separations >1 mm. At smaller separations the ambient torques on the pendulum were too large for this mode of operation. The second mode has the pendulum held in position using the control electrodes. A digital PID control loop applies voltages to either one or the other of the control electrodes so that the autocollimator reading remains essentially unchanged. The torque on the pendulum is proportional to the control electrode voltage squared. The voltage-to-torque calibration depends on the electrode and pendulum geometry. Therefore, we developed a technique which allows us to continuously monitor the instrument's calibration.

We rotate two ≈ 2.0 kg brass cylinders, around the pendulum outside the vacuum chamber, at constant frequency (2.48 mHz). The gravitational coupling between the pendulum and these masses produces small torques at twice and four times the rotation frequency. Since these calibration signals are at fixed frequencies, they do not affect the science data. To absolutely calibrate the electrostatic feedback torque we compare this gravitational torque signal to the same torque measured in the a free run method. The signal at four times per revolution was also calculated using the pendulum mass distribution.

There are two significant advantages to running the system in the feedback mode: (1) the dynamic torque range of the system is expanded by the gain of the feedback loop (≈ 1000) to $\approx 5 \times 10^{-10}$ Nm, and (2) the system recovers quickly from rare but large disturbances to the pendulum, such as earthquakes, fiber-quakes, or spontaneous

pressure spikes.

Torque sensitivity of our torsion balance

The noise performance of our torsion balance is best demonstrated by the power spectral amplitude of the torque noise when the pendulum is operated in the free running mode and with a large plate-pendulum separation. The torque spectrum is generated from the angular deflection spectrum by dividing by the pendulum's response function given by

$$r(f) = \frac{1/\kappa}{(1 - f^2/f_o^2) + i/Q}, \quad (1)$$

where f_o is the natural frequency and Q is the oscillator's quality factor $Q \approx 3000$.

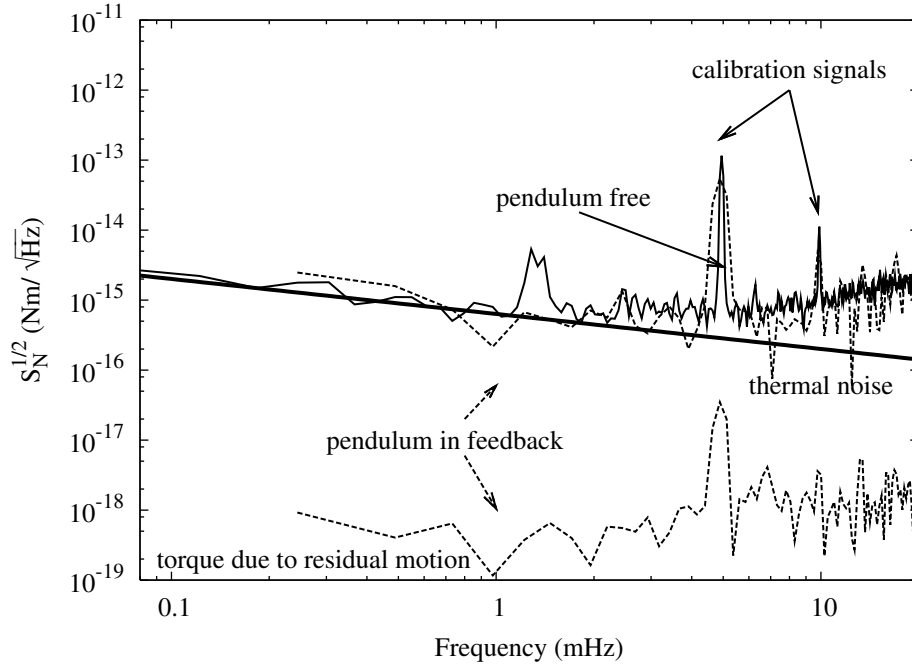


FIGURE 2. Performance of our torsion balance. The thick line presents the theoretical limit given by the thermal noise. The solid line is the measured power spectral amplitude of the torque in the free running mode. The dashed lines represent the torque noise for the system in the feedback mode. The upper dashed trace is the torque produced by the control electrodes and the lower trace is the torque stored in the fiber by the residual deflection of the pendulum. This data was taken at a plate-pendulum separation of 5 mm.

Figure 2 shows the power spectral amplitude of the torque as a function of frequency for a free running pendulum and for the pendulum in feedback. For the pendulum in feedback two traces are shown. The upper curve is the torque noise measured in feedback and the lower curve is the remaining torque in the fiber. At low frequencies, both measurement techniques reach the thermal limit of a torsion balance, given by

$$S_N^{1/2}(f) = \sqrt{\frac{4k_B T \kappa}{2\pi Q f}}, \quad (2)$$

with the Boltzmann constant k_B and the room temperature T [5]. At higher frequencies (> 5 mHz) the measured torque noise is in excess of the thermal noise due to autocollimator noise, typically $130 \text{ nrad}/\sqrt{\text{Hz}}$ at 6 mHz. The gravitational calibration signals can be seen at 4.95 mHz (Q_{22}) and 9.9 mHz (Q_{44}).

For purposes of comparison, we convert our measured torque noise spectra into acceleration noise spectra, which can be compared with LISA requirements. To convert torques into LISA-equivalent accelerations we use the expression

$$a = \frac{4\eta}{M} \frac{A}{l^2 h} N, \quad (3)$$

in which $M = 1.96 \text{ kg}$ is the mass of the LISA test mass and $A = 21.16 \text{ cm}^2$ is the surface area of one side of the cube, N is the torque, and η is a geometrical integration constant, for which a conservative value is two. Figure 3 shows the LISA-equivalent acceleration noise. At 1 mHz the acceleration noise of our apparatus is one order of magnitude above the LISA requirement. The torsion balance has its best performance at around 10 mHz, where the acceleration sensitivity is slightly better than the requirement.

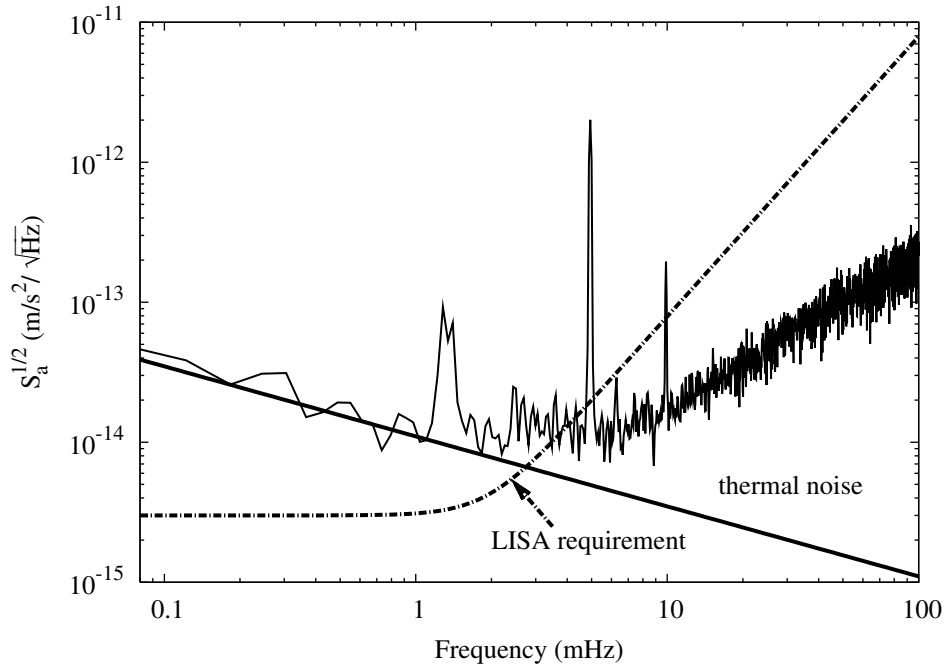


FIGURE 3. LISA-equivalent acceleration noise as a function of frequency. The thick solid line is the thermal limit for our torsion balance. The two sharp peaks correspond to our calibration signals.

Surface Potential

Fluctuations in the electrical surface potential differences (“surface potentials”) are one of the dominant noise sources at frequencies below 1 mHz. We can measure the surface potential between the pendulum and each half of the copper plates by using the

pendulum in feedback. The torque produced by a voltage applied to the copper plate is given by $c(V - V_{SP})^2$, where V_{SP} is the surface potential between the pendulum and the plate and c is a calibration constant, which depends on the plate-pendulum separation. Figure 4 shows a measurement of this relationship.

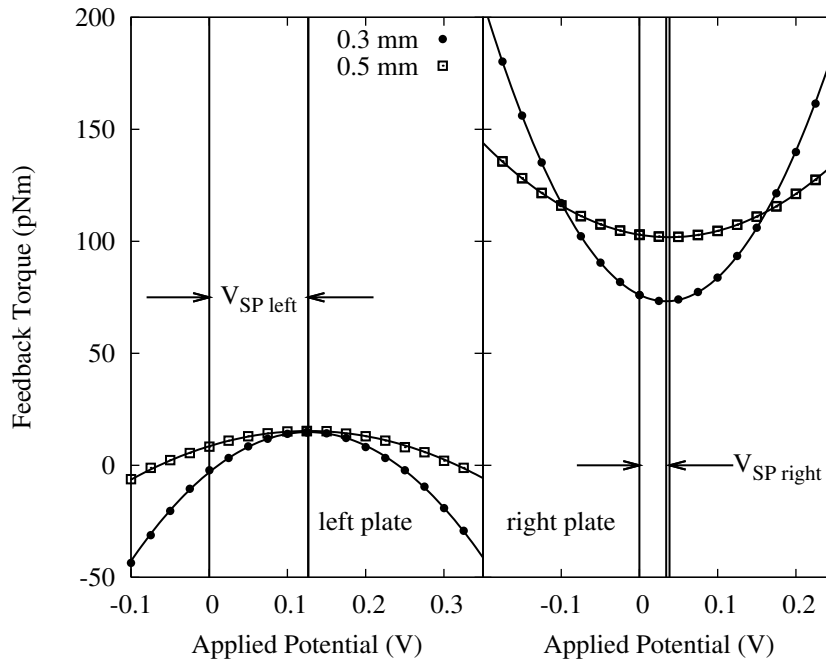


FIGURE 4. The measured torque as a function of potential applied to each half plate. The potential at the minimum of each parabola gives the surface potential.

We found that the surface potential is 0.13 V for the left plate and 0.03 V for the right plate. The measured values for the surface potentials are independent of the plate-pendulum separation. However, the surface potential was found to vary by ± 5 mV in a period of 150 days. After the investigation of thermal effects [4], the surface potential changed drastically by 50 mV. Most of this change occurred after the first heating cycle of the copper plate.

In order to investigate the temporal behavior of the surface potential fluctuations we alternate between two voltages V_1 and V_2 . V_1 and V_2 were applied for 500 s each and were chosen symmetrically around V_{SP} , so that the torque on the pendulum remains essentially constant and transients in the torques are minimized. From small differences in the measured torque, the voltage difference $V_2 - V_1$, and the calibration constant we calculate the surface potential. The power spectral amplitude of such a measurement is shown in Figure 5. The spectrum is white at a level of $\approx 200 \mu\text{V}/\sqrt{\text{Hz}}$ for frequencies below 0.1 mHz and therefore most likely determined by the sensitivity of our apparatus. However, there is a hint of increased surface potential fluctuation at frequencies below 0.1 mHz. This low frequency rise is found consistently in similar measurements.

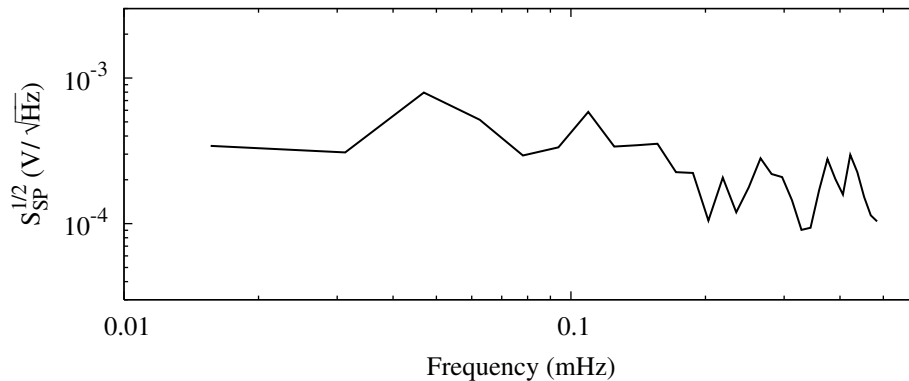


FIGURE 5. A typical measurement of the power spectral amplitude of the surface potential. This plot was generated from a 24 hour long run at a plate-pendulum separation of 0.3 mm.

CONCLUSION

We presented the specifications and capabilities of our high sensitivity torsion balance for LISA. In the absence of external forces (i.e. large separations) the torsion balance reaches the thermal limit given by the torsion fiber properties. At 1 mHz the LISA-equivalent acceleration sensitivity is only one order of magnitude higher than the LISA requirement. In addition, we have demonstrated that we can collect data in an electrostatic feedback mode, where the pendulum is held at a fixed angular position without increasing the noise. We have measured the surface potential using this feedback method. We were able to measure the fluctuation of the surface potential at sub-mHz frequencies. Currently, we are focusing our efforts on improving the sensitivity for time varying surface potentials.

This work was supported by the NASA contracts NAS5-03075, NNC04GBG03G and grant NNG05GF74G.

REFERENCES

1. P. L. Bender, K. V. Danzmann, and the LISA Study Team, *Laser Interferometer Space Antenna for the Detection of Gravitational Waves, Pre-Phase A Report*, Max-Planck Institute for Quantum Optics, Garching, Germany, 1998, MPQ-233 2nd edn.
2. DRS ITAT, *LISA DRS Acceleration Noise Budget*, LIST Working Group 3, 2005, January 25.
3. A. Hammesfahr, *LISA: Study of the Laser Interferometer Space Antenna, Final Technical Report*, ESTEC contract 13631/99/NL/MS, Astrium, 2000.
4. S. E. Pollack, S. Schlamminger, and J. H. Gundlach, “Outgassing, Temperature Gradients and the Radiometer Effect in LISA: A Torsion Pendulum Investigation,” in *Proceedings of the 6th International LISA Symposium*, American Institute of Physics, 2006.
5. P. R. Saulson, *Phys. Rev. D* **42**, 2437–2445 (1990).